TechS Vidya e-Journal of Research
ISSN 2322 - 0791
Vol. 2 (2013-14) pp. 4-23.

Synthetic Aperture Radar

Mannil Mohan

Department of Applied Sciences
Vidya Academy of Science & Technology
Thrissur - 680501, India
email:mannil.m@vidyaacademy.ac.in

Abstract: Synthetic Aperture Radar (SAR) is a microwave radar which combines all weather operation and very high resolution through aperture synthesis to become a unique remote sensing device for monitoring the earth's surface from orbiting satellites. This article discusses the basic principles behind how a SAR achieves high resolutions in the range and azimuthal directions from a high altitude moving platform to image the earths surface in terms of microwave backscattering cross section. Furthermore, the unique data processing employed by SAR enables the determination of velocities of moving objects and detection of land and oceanographic subsurface phenomena. Examples of applications of SAR are also presented.

1 Introduction

All radars are active remote sensing devices with their own sources of electromagnetic waves (in radio or microwave frequencies) for illuminating a target. The specific advantage of using microwaves for remote sensing is their ability to penetrate clouds and haze in the atmosphere enabling remote sensing operations under all weather conditions. Microwaves with frequencies in the range 1 to 40 GHz (corresponding to wavelengths 30 to 0.75cm) are considered the most suitable particularly, for studying oceanographic phenomena using airborne and space-borne radars. Above 40 GHz,the observations start getting affected by atmospheric absorption by water vapour and oxygen while below 1GHz, there are problems of poorer spatial resolution, interferences from anthropogenic radio signals and galactic microwave noise[1,2].

Among different types of radars, synthetic aperture radar (SAR) has the unique capability of observing the earth's surface with resolutions better than 5 m even through layers of clouds from the high altitudes of satellites like 600 to 1000km. Since their first experimental demonstration in 1953, a number of SARs have flown on board several aircrafts and satellites (SEASAT SAR, Shuttle Imaging Radars-SIR A, B & C, ERS SAR, Radarsat, RISAT-1 & 2, etc.)[3] and have amassed a wealth of information valuable for studies in

TechS Vidya e-Journal of Research
ISSN 2322 - 0791
Vol. 2 (2013-14) pp. 4-23.

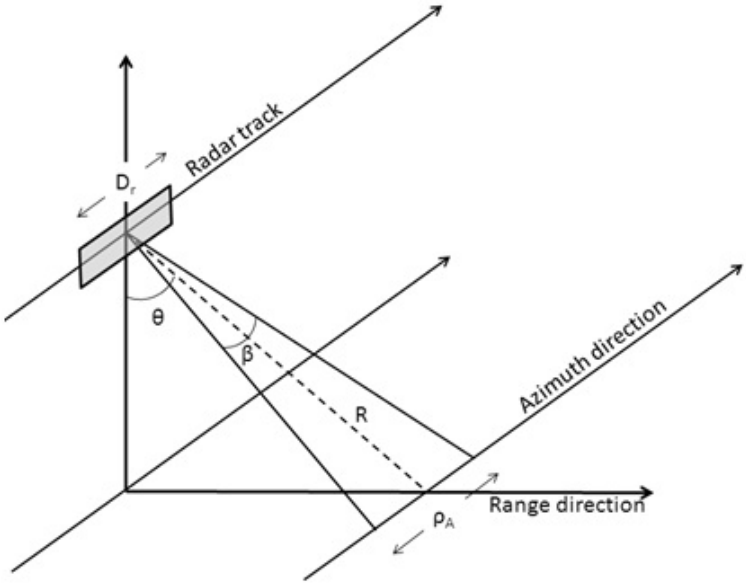

Figure 1: Beamwidth geometry of a Real Aperture Radar (RAR)

geology, hydrology, forestry, ocean waves, coastal bathymetry, oceanic current systems, oil slick detection, etc. The high resolution and the exclusive observation technique employed by SAR have brought out several features over land and oceans (e.g. subterranean extinct river beds in the Sahara desert, internal gravity waves in the Andaman seas, etc.) previously not realisable by any other remote sensing methods. However, the complex nature of SAR image formation with its inherent nonlinearity is still not fully understood making it an active field of research in microwave remote sensing. An example is the correct delineation of oceanographic features in a SAR image of a rough sea surface under a heavy storm which is a quite difficult problem.

In the following sections, we discuss the basic principles of SAR, the associated data processing, ocean wave imaging and its oceanographic and coastal applications.

2 Principles of Synthetic Aperture Radar

The high resolution potential achieved by SAR can be understood by first going through the resolution of a Real Aperture Radar (RAR). As illustrated in Figure 1, it is convenient to define the two dimensional ground surface scanned by a high altitude flying RAR in terms of along-track and across-track directions, also known as azimuthal and range directions respectively.One defines the diffraction limited beam width of the radar in the azimuthal

direction [4] as

$$\beta = \frac{\lambda_r}{D_r} \tag{1}$$

where λ_r is the operating wave length and D_r is the antenna aperture size. The azimuthal ground resolution at a slant height R is therefore

$$\rho_r = \beta R = \frac{\lambda_r R}{D_r}. \tag{2}$$

Accordingly, for a λ_r between 5 cm (C-band microwave) and 30 cm (L-band microwave), to obtain a ground resolution of 5 m for an RAR mounted on an aircraft flying at an altitude $\sim$4 km, the required antenna size is 10 to 60 m. To achieve the same resolution from a satellite at an altitude $\sim$750 km, the antenna size has to be 7.5 to 45km! This is clearly impossible with the current space technology.

SAR overcomes the above difficulty through a technique of coherent processing of the reflected microwave signals collected over a long stretch of distance along its track resulting in an effective increase in the antenna size, to achieve the desired resolution. The method of coherent processing of the signals collected by the radar over the long distance it travels during the up and down flight time of a microwave pulse effectively 'synthesizes' a virtual antenna of the same size. This results in a tremendous (typically, $\sim 10^3$ to 10^4 times)increase in the resolution in the azimuthal direction. Along with this, a pulse compression technique is also put in place to attain high resolution in the range direction. These two techniques are described below.

2.1 Range resolution

Let us consider range resolution at first. In the case of an RAR, the radar emits a pulse of pulse width τ at time $t = 0$ in the slant range direction to illuminate the ground (see Figures 2). The swath (the span of ground range) is usually kept very large (typically, $\sim$ 100 km) by having a wide beam width in the range direction. Some time after the emission of the pulse, return signals start arriving at the radar from the nearest point at distance R_n to the farthest point at distance R_f in a continuous stream, from time t_n ($= (2R_n)/c$, c being the velocity of light) to t_f ($= (2R_f)/c$). The time history of signal intensity during this period will be a convolution of the pulse width with the backscattering cross sections of the points on the ground from R_n to R_f. As the pulse shape is known accurately, the image of the ground in terms of the back scattering cross sections of the points is retrieved through the inversion of the time record of the return signal. The best range resolution that can be realized by an RAR is

$$\rho_R = \frac{c\tau}{2\sin\theta} \tag{3}$$

where θ is the average angle made by the slant range with the vertical. For a pulse of typical width $\sim$30 μs and $\theta \sim 45^\circ$, ρ_R is $\sim$3 km. Hence in order to get a range resolution of say, $\sim$5 m, a pulse of extremely narrow width has to be employed which is impractical. In the case of SAR, this is realized through a technique of pulse compression known as "chirping"

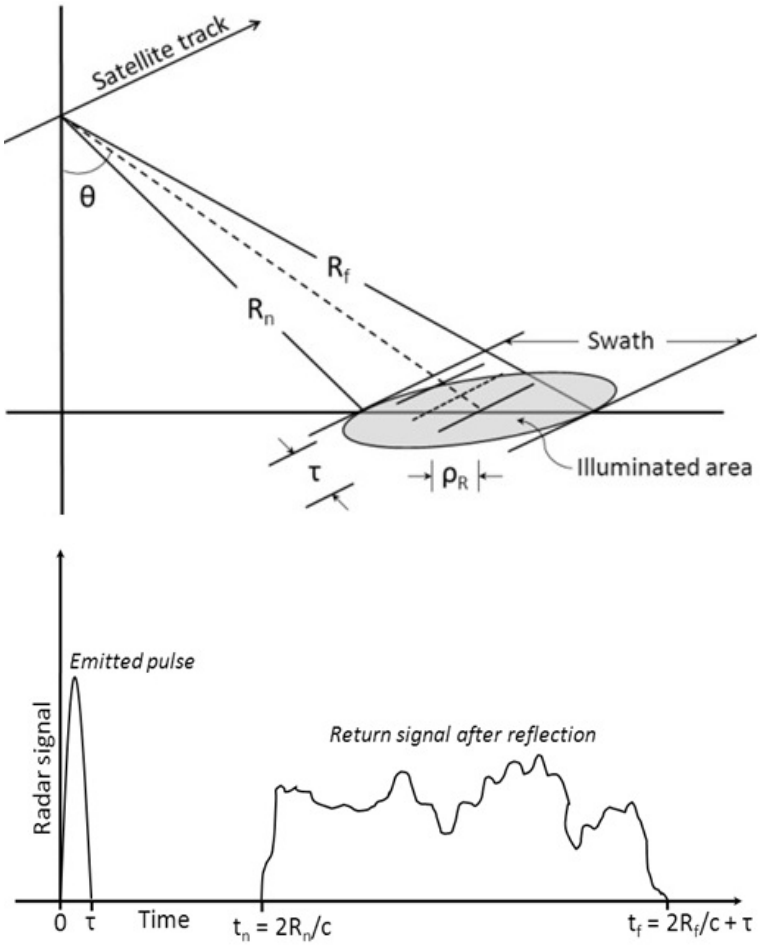

Figure 2: Geometry of the range resolution of a SAR)

[4,5]. Chirping consists of decreasing the frequency f of the radar through a bandwidth δf with in each pulse (Figure 3). Then the reflected signals are subjected to a process of matched frequency filtering which effectively narrows down the pulse width by a factor $\tau\delta f$ (typically, $\sim$100) [4, 5].

A simpler way of viewing the range compression technique is illustrated in Figure 4. Between the leading and trailing edges of every pulse, the radar frequency decreases linearly from $f + \delta f/2$ to $f - \delta f/2$. As a result, for a pulse emitted at $t = 0$, the reflected signal received from a target point A on the ground also undergoes a frequency decrease from $f + \delta f/2$ to $f - \delta f/2$ during the interval t_1 ($= (2R_A)/c$) to $t_1 + \tau$. By matching the return signal during this period with a chirped reference signal identical to the emitted pulse, one can filter in the information about A. Only contributions from A will add up constructively while those from all other points will cancel out destructively. As the matched

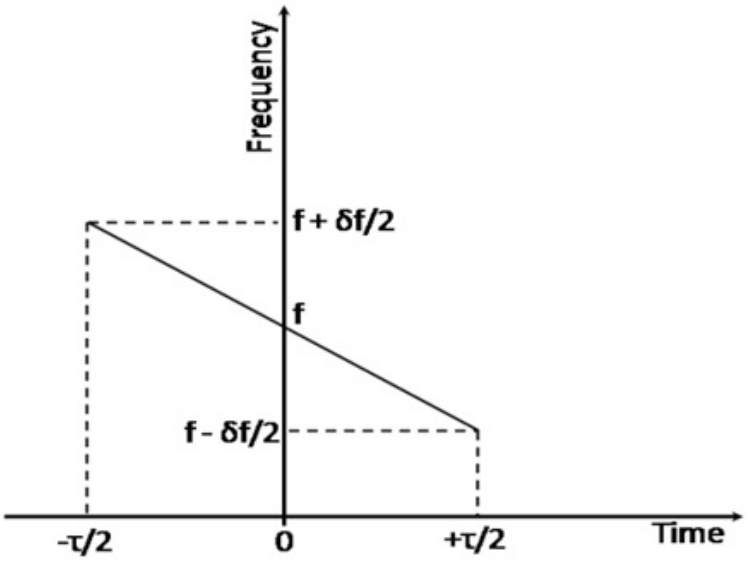

Figure 3: Frequency chirping within a pulse of width τ

filtering advances in time, backscatter information from other range points like $B, C, \ldots$ are obtained sequentially.

2.2 Azimuthal resolution

For the sake of the discussion here, we assume that the range processing of the radar signals has already been done as described in the previous section. So, let us next consider azimuthal resolution.The target points $a, b, c, \ldots$ as shown in Figure 5 are at a constant range, R. When the radar antenna moves forward, the point 'a' on the ground will remain within its beam width β for a duration

$$T = \frac{\rho_A}{V_A} \tag{4}$$

where ρ_A is given by Eq.(2) and V_A is the velocity of the radar. In the technique of aperture synthesis, the amplitudes and the phases of the reflected pulses from the point 'a' collected during T (called the integration time) are processed coherently to build a high resolution image of 'a' [4, 5, 6].

Since the distance moved by the radar during the time T is also ρ_A, it turns out to be the effective size of the antenna, or rather the size of the "synthesized" aperture. The resolution is therefore,

$$\rho_A^s = \frac{\lambda_g R}{2\rho_A}. \tag{5}$$

The factor 2 in the denominator here is due to the two way path of the microwave pulse, as

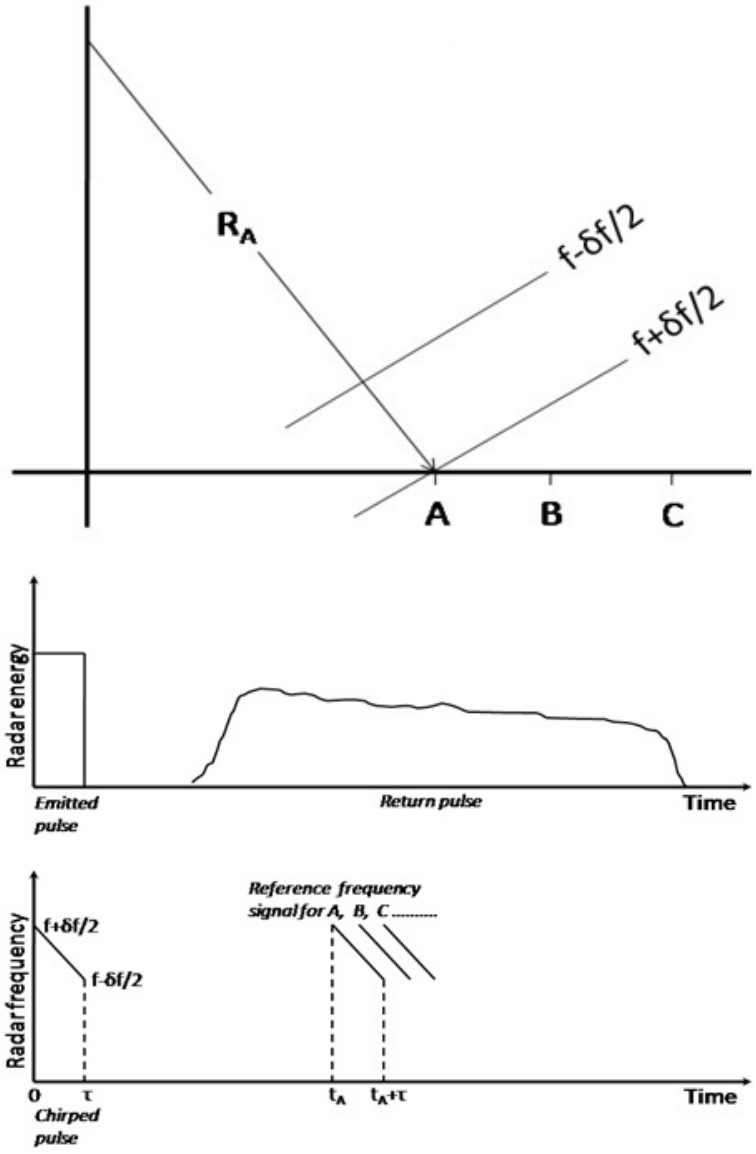

Figure 4: Frequency chirping and matched frequency filtering

the radar is an active instrument. Substituting for ρA from Eq. (2),

$$\rho_A^s = \frac{D_r}{2}. \tag{6}$$

This is an unexpected result! That is, the azimuthal resolution is independent of range and operating wave length and improves with the decreasing size of the antenna. The reason

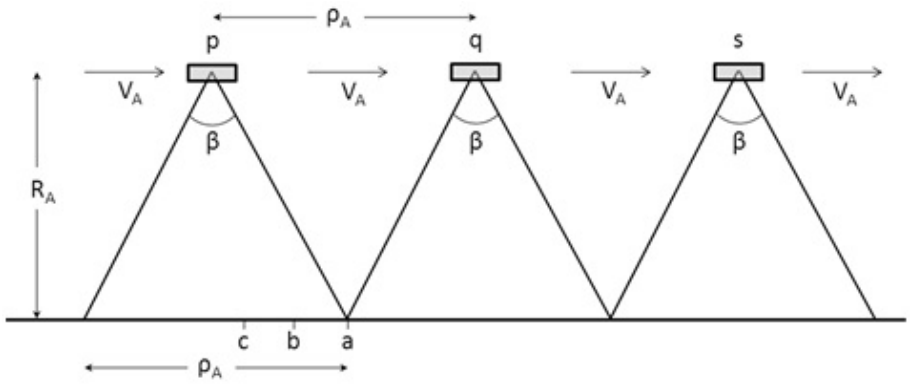

Figure 5: Azimuthal resolution geometry of SAR

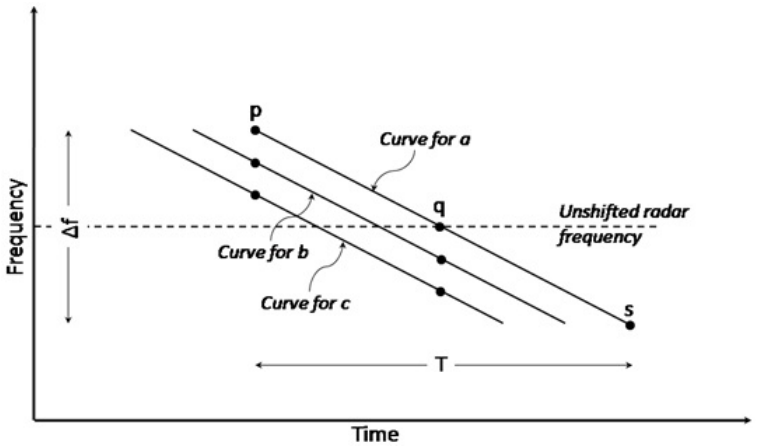

Figure 6: Doppler history curves for the ground points $a, b, c, \ldots$

lies in the fact that an increase in either the range or the radar wavelength enhances the integration time T and therefore the size of the effective aperture, allowing more information to be collected from a point on the ground which compensates exactly for the deteriorating effects of the increased beam width and the increased range.

But how to separate out the reflected pulses coming from different points on the ground lying at the same range? The answer lies in the uniform azimuthal motion of the radar which produces a steady, linearly decreasing Doppler shift in the reflected signals from these points. For instance, when the radar moves from position 'p' to position 'q' in Figure 5, the ground point 'a' moves radially inward towards the radar resulting in a positive Doppler shift or an increase in reflected frequency. This Doppler shift reduces to zero as the radar reaches the position 'q' where the radial velocity is zero and from then onwards to

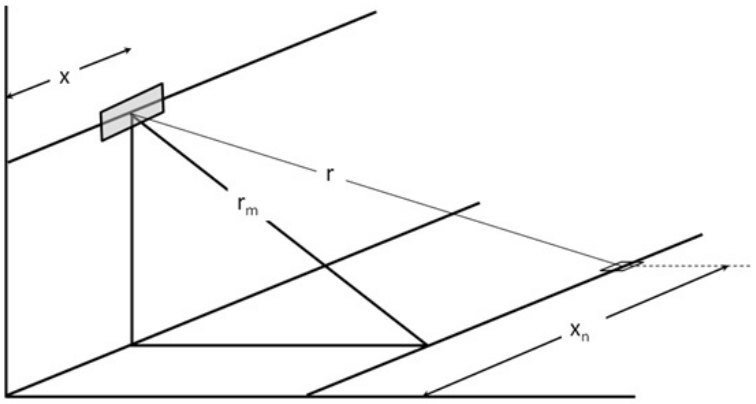

Figure 7: Position of ground resolution cell at (x_n, r_m) with respect to SAR

the position 's', the point 'a' moves radially outwards causing a linearly increasing negative Doppler shift. Or alternately, at the position 'p', the radar receives the reflected signals from $a, b, c, \ldots$ with linearly decreasing Doppler shifts from a positive value to a negative value since each point is at a different stage of its individual "Doppler history". This offers a unique means to identify each point lying at a constant range. The Doppler history curves of the return signals from $a, b, c, \ldots$ are plotted in Figure 6. It must however be noted that there will not be a continuous set of curves covering all the ground points due to the discrete nature of the pulses. The curves will be closely placed but separated. One can see that each of these curves is quite similar to the return signal of a chirped pulse described in the range compression technique discussed in the previous section. Hence in the same way,the high resolution information from each ground point can be filtered in by matching the reflected signals with a properly timed reference signal having pre-adjusted Doppler shifts. As in the case of range resolution, the aperture synthesis technique improves the azimuthal resolution by the factor $T\Delta f$ (typically, $\sim$500) where Δf is the Doppler frequency bandwidth.

3 Processing of SAR signals

As shown in Figure 7, the reflected signal received by SAR at time t and position x from a resolution cell on the ground at azimuth x_n and range r_m [4, 5, 7] is

$$s_{nm}(t) = \sigma(x_n, r_m) \exp\left[i\Omega\left(t - \frac{2r}{c}\right)\right] \tag{7}$$

where $\sigma(x_n, r_m)$ is in general a complex quantity containing information about the phase and amplitude of the reflected signal as well as the radar backscattering cross section at (x_n, r_m). The quantity Ω ($= 2\pi f = 2\pi c/\lambda_r$) is the angular frequency of the microwave. Since the SAR altitude is very high, one can assume $(x_n - x) \ll r_m$ and approximate r as

$$\begin{aligned} r &= \sqrt{r_m^2 + (x_n - x)^2} \\ &\approx r_m + \frac{(x - x_n)^2}{2r_m} \\ &= r_m + \frac{(V_A t - x_n)^2}{2r_m}. \end{aligned} \tag{8}$$

The total signal received by SAR from all the cells within its azimuthal beam width and the range interval (swath) is therefore

$$S(t) = \sum_{n,m} \sigma(x_n, r_m) \exp\left[i\left(\Omega t - \frac{4\pi r_m}{\lambda_r} - \frac{2\pi(V_A t - x_n)^2}{\lambda_r r_m}\right)\right] \tag{9}$$

SAR processing is mainly the inversion of Eq.(9) to retrieve (x_n, r_m) and from it, the backscattering cross sections of the resolution cells from $S(t)$ data[4, 5, 7].

A SAR on board an orbiting satellite records extremely large amounts of data. The data volume will be so huge that the processing will consist of generating the scattering cross sections of typically, millions of ground cells each second. Satellites in general, will not have computation facilities on board to perform this tremendous task and so, the collected data is down loaded in real time and the processing is done at ground stations.

4 Effects of target motion on SAR imaging

The SAR technique discussed above assumes that the target points on the ground are stationary. But if there are moving objects on the ground, SAR imaging becomes complicated. The most important effects produced by moving objects are discussed below.

4.1 Azimuthal shift

This effect arises from the motion of an object with a velocity component in the range direction. If the motion is in the positive range direction, the radar return signals undergo additional frequency decrease causing the whole Doppler history to shift so as to make the object appear at an earlier azimuthal location in a SAR image. If U_R is the range velocity, the corresponding azimuthal displacement is

$$\delta x = -\frac{U_R R}{V_A} \tag{10}$$

4.2 Range walk

In case U_R in Eq. (10) is very large, then the object may shift through one or more resolution cells within the integration time T. This will smear the objects image through the cells it has moved accompanied with a reduction in intensity. This effect is known as range walk and the condition that it does not occur is

$$|U_R| < \frac{\rho_R^s}{T} = \frac{2\rho_A^s \rho_R^s V_A}{\lambda_r R} \tag{11}$$

4.3 Azimuthal defocusing

Movements in the azimuthal direction can also interfere with the Doppler history leading to an azimuthal blurring of the image. This is known as azimuthal defocusing and the essential condition that it does not occur is

$$|U_A| < \frac{2\left(\rho_A^s\right)^2 V_A}{\lambda_r R} \tag{12}$$

where U_A is the target azimuthal velocity.

5 Speckles in the SAR image

An unavoidable consequence of image recording using a coherent source like SAR (or laser) for illumination is the appearance of speckles in the image. Speckles are grainy, random intensity variations superimposed on a normal image. It is caused by the random phase shifts the rough surface of a target imparts on the reflected electromagnetic waves. Such phase shifts result in constructive interference of the waves from some of the resolution cells while destructive interference of the waves from some other cells. As a consequence, random intensity fluctuations or speckles appear as an additional feature superimposed on the normal image.

One way to reduce speckles is through a procedure of image averaging even though it degrades the resolution to some extent. For instance, if the signals collected over one fourth of the synthetic aperture length is processed,the image resolution will degrade by a factor of four. By dividing the synthesized aperture into four equal parts and processing the corresponding data separately, one obtains four independent "looks" of the same scene contaminated with speckles. Since the phase fluctuations produced by target surface vary very rapidly with time and look angles, the speckles will be randomly located in the images. These uncorrelated speckles are then removed by averaging the four images.

6 Ocean wave imaging by SAR

Ocean surface imaging is a very important oceanographic application of SAR. Even though SAR's capability for detecting ocean surface waves is fully recognized now, the actual physical mechanisms behind the imaging of a rapidly changing ocean surface are still not understood well and is an active research area.

Waves on an ocean surface at any time, are distributed over a wide range of wavelengths; from the very small capillary waves or ripples ($\lambda \sim$a few cm) to very long swells ($\lambda \sim$100 m). In the microwave remote sensing of ocean waves, a commonly accepted representation of ocean surface is the two-scale roughness model which divides the whole wave spectrum into two regions. One is the short wavelength capillary waves region responsible for the radar backscatter via Bragg resonance and the other is the long wavelength swell region

which modulates the backscatter intensity through various mechanisms. Such modulation mechanisms in general, are common to all types of radar imaging.

The radar backscatter intensity from a rough ocean surface is given by [4, 5, 7, 8]

$$\mu(x) = \mu_0 \left[1 + \iiint \left(R(\mathbf{k_s}) Z(\mathbf{k_s}) e^{(i(\mathbf{k}\cdot\mathbf{x} - \Omega t))} + \text{complex conjugate} \right) d^3\mathbf{k_s} \right] \quad (13)$$

where $\mathbf{k_s}$ is the ocean surface wave vector, $R(\mathbf{k_s})$ is the modulation transfer function (MTF) and $Z(\mathbf{k_s})$ is the Fourier transform of the ocean surface elevation associated with the swell waves. One can see here that the role of MTF is to translate large scale ocean surface features into a radar image in terms of backscatter intensity variations.

6.1 Contributions to MTF

Contributions to MTF usually come from two sources: tilt modulation and hydrodynamic modulation described below [4, 8].

(a) **Tilt modulation**: This mechanism represents μ variations arising from the tilting of sea surface by long wavelength swells. The gradually varying sea surface tilts due to long wavelength swells produce a corresponding gradient in the local incident angle of the radar pulses. This causes the Bragg scatter intensity variations with wavelengths exactly same as those of the swells (Figure 8). The Bragg scatter is stronger from the portions of the swell wave surfaces (called facets) facing the radar and weaker from those facing away.Tilt modulation effect is maximum for swell waves traveling in the range direction and it is very small or nearly absent for waves traveling in the azimuthal direction.

(b) **Hydrodynamic modulation**: The wave-wave interactions between the short wavelength ripples and the long wavelength swells tend to accumulate the short wavelength waves at the crests of the swells (Figure 8). This is because of the alternate convergent and divergent surface currents associated with the swells which advect the ripples to the crests. Accordingly, the Bragg scatter intensity will also be modulated with the same periodicity as that of the swells. But this process becomes very complicated in stormy seas when the wave amplitudes are very high and the nonlinear wave-wave interactions are much stronger. For low wave amplitudes, hydrodynamic modulation is absent when ripples and swells travel at 90° to each other.

6.2 Velocity bunching

Besides the above modulation mechanisms, SAR imaging suffers from additional azimuthal displacements caused by the up and down fluid motions associated with the swells [4]. This phenomenon, called "velocity bunching" can also be characterized mathematically by a transfer function in a similar way as the tilt and hydrodynamic modulations. As illustrated

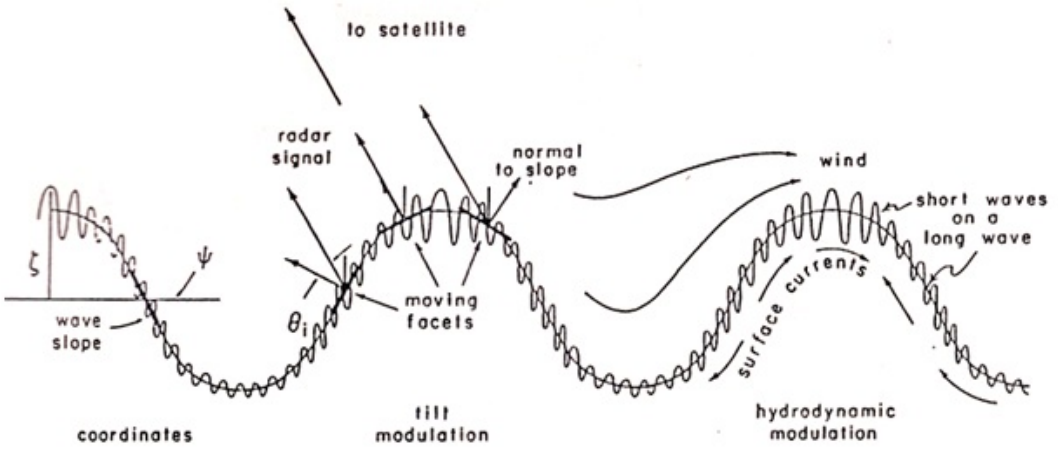

Figure 8: Tilt and hydrodynamic modulations produced by long wave lengths swells (Courtesy: Robinson, 1985)

in Figure 9, a sinusoidal swell propagating in the azimuthal direction has opposing fluid movements at the rising and falling facets of the wave. This asymmetry leads to opposite azimuthal shifts on either side of a crest or a trough distorting the image intensity variation into a non-sinusoidal pattern. If the waves in a SAR image are of low amplitude, the distortions are not very severe and the image can still be used to derive information about wavelengths and swell directions. But if the swell waves are strong, the azimuthal shifts start to overlap with each other making the velocity bunching highly nonlinear making the image interpretation very difficult. For an azimuthal shift of magnitude $|U_R/V|$, the parameter controlling the linear limit of velocity bunching is,

$$C_{vb} = \frac{R}{V}\frac{d\langle U_R\rangle}{dx_0} \tag{14}$$

where $\langle U_R\rangle$ is the range velocity of the surface facets averaged over the SAR integration time T and x_0 is the azimuthal coordinate in the ocean surface plane. If $|C_{vb}| < 0.3$, velocity bunching effect may be considered linear. However, for waves traveling in the range direction, the azimuthal shifts are parallel to the wave fronts producing no image distortion.

6.3 Conditions for wave imaging by SAR

Oceanic SAR images need not always show the presence of waves. There are certain minimum conditions a wave field should satisfy to show up in a SAR image. These are:

(a) Sea surface wind u_{10} (defined as the wind at 10 m height from sea surface) must exceed 2 to 3 m/s so that sufficient amount of short waves or capillary waves is

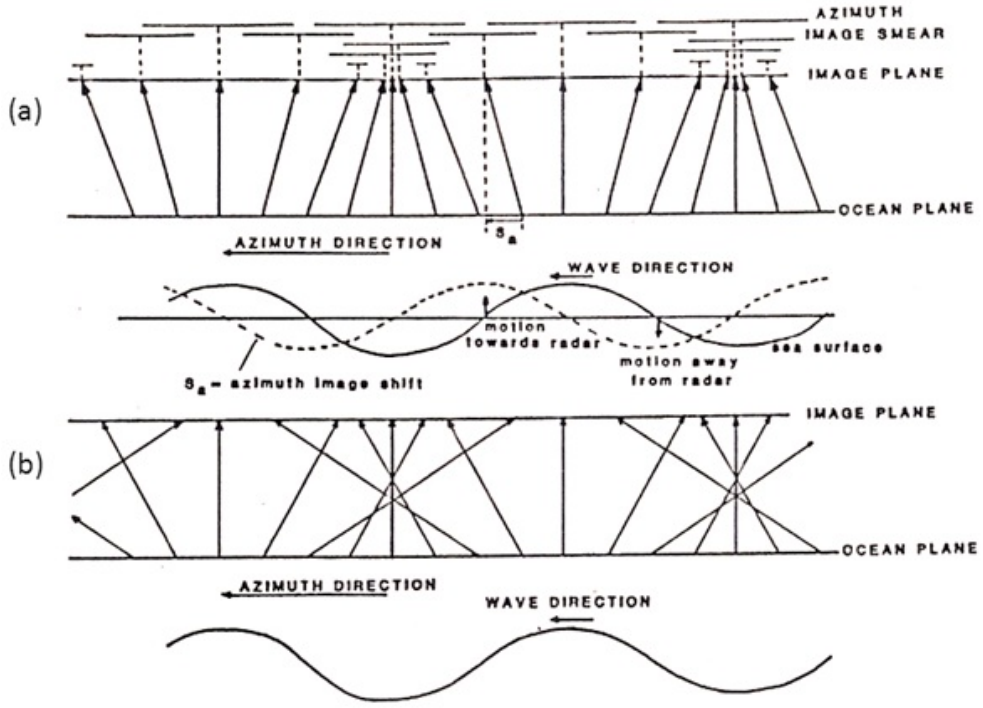

Figure 9: (a) Non uniform azimuthal shifts due to velocity bunching (b) Nonlinear velocity bunching due to high wave amplitude (Courtesy: Robinson, 1985)

generated. In the absence of short waves, radar signals cannot not undergo Bragg scatter which will lead to a darkening of the image.

(b) (b) The wavelength of a wave must exceed twice the size of a ground resolution cell (Nyquist sampling criterion).

(c) The significant wave height $H_{(1/3)}$ of the long wavelength swells on the sea surface must exceed $\sim$1.4 m.

7 Oceanographic applications

The correct retrieval of sea surface parameters from SAR data is still not a fully solved problem. The difficulties mainly originate from the complexities of the modulation transfer and velocity bunching mechanisms which map the ocean surface into a SAR image particularly, at high sea states conditions. Nevertheless, more often than not, oceanic SAR images do display waves and several wavelike features very clearly. Careful examination of these features can yield a wealth of oceanographic information. Some of them are described below.

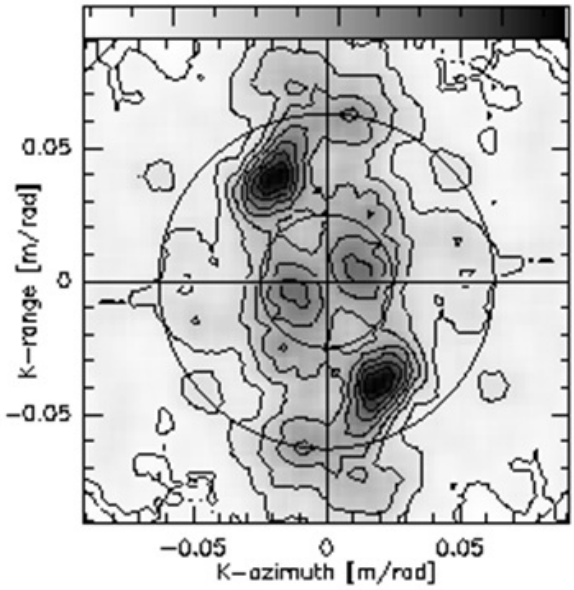

Figure 10: 2D-FFT directional wave spectrum of an ERS-1 SAR wave image (Courtesy: Corsini, et al., 2014)

7.1 Directional wave spectrum

One of the very significant applications of SAR is the retrieval of ocean surface wave information. A wave field in general, consists of a superposition of several waves with different wavelengths and different directions of propagation. The best way of deriving wave information from a SAR image is through a two dimensional fast Fourier transform (2D-FFT) [9]. All the major waves in a wave field can be identified as maximum intensity peaks in the 2D-FFT power spectrum of the image. Figure 10 is a typical 2D-FFT power spectrum of a SAR wave image [9]. The spectral peaks shown as dark patches represent the main waves. The radial distances of the peaks from the centre give the wave numbers ($= 2\pi/\lambda$, where λ is the wavelength) while their angular positions with respect to the horizontal give the propagation directions.

However, the wave information derived from a SAR image need not be the exact representation of a wave field because of the distortions introduced by the modulation and velocity bunching effects. In certain cases, depending on the wave amplitudes and propagation directions, the 2D-FFT spectrum can be corrected for these distortions with properly chosen mathematical transformations. But in high seas, where the wave amplitudes are very high, identifying the right type of transformations is very difficult.

7.2 Shallow water bathymetry

Sea surface waves propagating towards a coastal line undergo a decrease in wavelength and refraction of direction if the angle of incidence is oblique. This phenomenon can be utilized to estimate coastal ocean depths whenever a series of waves are clearly seen in a SAR image. The dispersion relation of surface gravity waves in shallow water [10] is

$$\omega^2 = \frac{2\pi}{\lambda} g \tanh\left(\frac{2\pi}{\lambda} h\right) \tag{15}$$

where ω is the angular frequency of the wave, λ is the wavelength, g is the acceleration due to gravity and h is the water depth. A wave traveling from deep ocean towards the shore maintains the same frequency but undergoes a change in wavelength as

$$\frac{2\pi}{\lambda_0} = \frac{2\pi}{\lambda_1} g \tanh\left(\frac{2\pi}{\lambda_1} h_1\right) \tag{16}$$

where λ_0 is the wavelength in deep ocean and λ_1 is the wavelength at depth h_1. Thus by measuring the wavelength of a shore-ward propagating long wavelength wave at different points, the corresponding ocean depths can be determined from Eq. (16) as

$$h_1 = \frac{\lambda_1}{2\pi} \tanh^{-1}\left(\frac{\lambda_1}{\lambda_0}\right). \tag{17}$$

2D-FFT is an effective method for the accurate estimation of wavelengths and propagation directions of waves in a SAR image. But since SAR images most often contain a mixture of several waves, it may lead to some confusion in keeping track of each wave from deep ocean to the coast. To avoid this, a spatially continuous chain of smaller sub-images is defined in the original SAR image with sufficient overlaps and each image is 2D-FFT analysed to determine the gradual changes in wavelengths and wave directions.

7.3 Estimation of rotational velocity of gyres

On some occasions, large scale circular current systems called gyres occur in certain parts of the sea. The current velocities in these gyres distort their appearance in SAR images from circles to elliptical shapes (Figure 12). This distortion is a result of the non-uniform range component of the fluid velocity around a circular gyre, giving rise to non-uniform azimuthal shifts. The maximum azimuthal shift for a gyre rotating with a tangential velocity v is

$$|\delta x| = \frac{v}{V_A} h_s \tan\theta \tag{18}$$

where h_s is the satellite altitude and θ is the angle made by the slant range with the vertical. As shown in Figure 11, a gyre image may be azimuthally compressed or elongated depending on whether the rotation is clockwise or anti-clockwise. The relationship (18) can therefore be used to determine the speed and direction of a rotating gyre in a SAR image from its azimuthal compression/elongation.

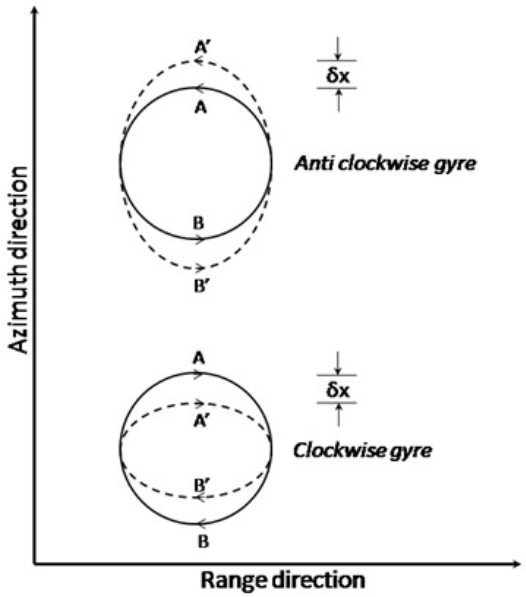

Figure 11: Deformations of clockwise and anti clockwise rotating gyres in a SAR image

7.4 Internal gravity waves

These are subsurface long wavelength (several hundred meters to several kilometers) internal gravity waves generated by perturbations at the thermocline interface (10 to 200m deep) which separates the warm upper layer of ocean water from the cold, denser lower layers [4, 8]. The fluid particle velocity fields associated with internal waves produce alternately convergent and divergent current zones (Figure 12) at the sea surface which advect the surface roughness into periodic bands of high and low intensities. These roughness modulations having the same wavelengths as that of the internal gravity waves can be detected by a SAR. Thus SAR has the capability to detect even subsurface oceanic phenomena through their feeble signatures on the sea surface roughness.

Internal waves are seen frequently in SAR images of ocean surface in the vicinity of sea mounts, over the edges of continental shelves and at places of current shear. Figure14 shows internal waves detected by ESA-Advanced SAR in the Andamans Sea.

7.5 Other applications of SAR

In addition to the ones discussed above, SAR has demonstrated its potential for many other useful applications. Some of them are mentioned here:

(a) Using mutifrequency microwave signals along with polarimetry, SAR has demonstrated the capability to distinguish different types of sea ice (Figure 14), for instance, between one year and older ice.

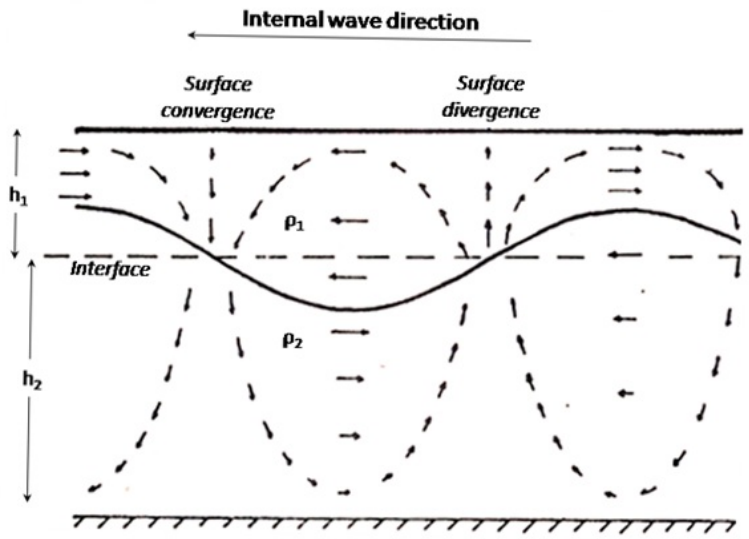

Figure 12: Diagram of an internal gravity wave with the associated fluid particle velocity field (Courtesy: Robinson, 1985)

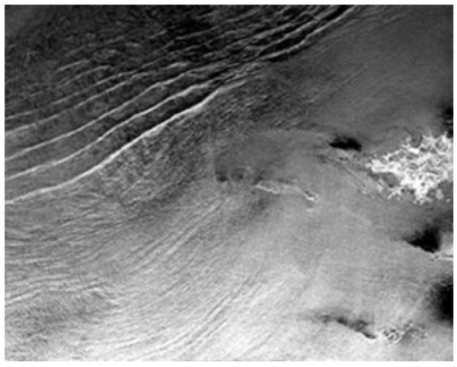

Figure 13: ESA-Advanced SAR image of internal waves in the Andamans sea (Courtesy: www.esa.int)

(b) Oil slicks floating on the sea surface reduce the surface roughness by suppressing capillary waves and thereby, the Braggscatter intensity. This helps in the detection of oil slicks as dark patches in SAR images (Figure 15)

(c) In a SAR image,the Doppler shift caused by the motion of a ship makes it appear azimuthally displaced with respect to the wake left behind on the sea surface (Figure 16). By measuring the displacement of the ship and from the orientation of the wake, the ship's speed and direction can be determined.

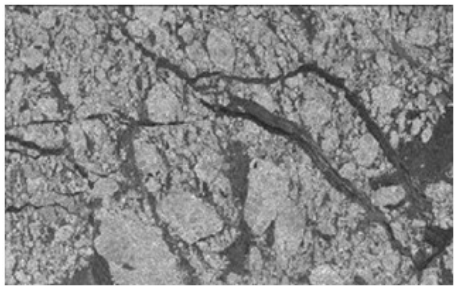

Figure 14: Sea ice detected by RADRSAT near Alaska. In the brightness gradient, older, thicker layers of ice appear whiter in this SAR image (Courtesy: www. nsidc.org)

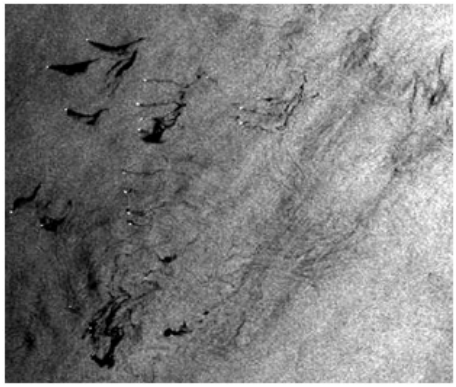

Figure 15: Oil drilling field with in the North Sea several oil slicks detected by ESA-ERS SAR (Courtesy:www.earth.esa.int)

8 Conclusions

SAR achieves very high resolution for microwave remote sensing through: (i) "chirping" of the emitted pulses in the range direction and, (ii) the "synthesis" of a virtual aperture over the distance the radar moves in the azimuthal direction during the up and down travel of a pulse. The reflected microwave signals are collected using matched filters and coherently processed to create an image in terms of the backscattering cross sections of the ground resolution cells. In addition to achieving very high resolution and all weather capability, the specialized data processing employed by SAR enables the determination of velocities of moving objects, study of oceanographic internal gravity waves, and detection of subsurface drainage systems over deserts. A number of SARs have been flown onboard earth observing satellites over the past $\sim$30 years by international space agencies like NASA, Roscosmos, ESA, ISRO, JAXA, CNSA, etc. which have brought out several unknown aspects of the earth's surface over the land and the oceans.

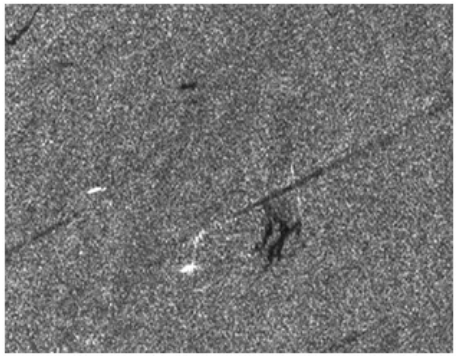

Figure 16: ESA-ERS SAR image of two ships moving in opposite directions in Malaca Strait. The displacements from their wake correspond to their velocities in the range direction. (Courtesy: www.crisp.nus.edu)

References

[1] V. J. Falcone, Jr., L. W. Abreu, and E. P. Shettle, "Atmospheric attenuation in the 30 to 300 GHz region using RADTRAN and MWTRAN", Proceedings of the Meeting, Arlington, VA, May 6-7, 1982, SPIE - The International Society for Optical Engineering, 1982, 62-66, 1982.

[2] T. Oguchi,"Electromagnetic wave propagation and scattering in rain and other hydrometeors", IEEE, Proceedings (ISSN 0018-9219), vol. 71, 1029-1078, Sept. 1983.

[3] C. Elachi, W. E. Brown, J. B. Cimino, *et al*, "Shuttle Imaging Radar Experiment," Science, 3, Vol. 218, No. 4576, 996-1003, DOI: 10.1126/science.218.4576.996, December 1982.

[4] I. S. Robinson, "Satellite Oceanography", Ellis Horwood Ltd. and John Wiley & Sons, Chichester, West Sussex, England, 1983, 344-394, 1985.

[5] T. D. Allen, "Satellite Microwave Remote Sensing", Ellis Horwood Ltd. and John Wiley & Sons, Chichester, West Sussex, England, 107-305, 1983.

[6] L. J. Cutrona, "On the application of coherent optical processing techniques to Synthetic Aperture Radar", Proceedings of the IEEE, Volume:54, Issue: 8, 1026 1032, Aug. 1996.

[7] L. J. Cutrona, "Synthetic Aperture Radar", in Radar Handbook, second edition, Ed. M. Skolnik, McGraw-Hill, New York, 1990.

[8] R. H. Stewart, "Methods of Satellite Oceanography", University of California Press , Los Angeles, 85-107, 1985.

[9] R. Corsini, R. Grasso, G. Manaraand, A. Monorchio, "Estimation of directional sea spectra from ERS/SAR images of Mediterranean areas: A case study", https://earth.esa.int/workshops/ers97/ papers/corsini/, 2014.

[10] A. Sommerfeld, "Mechanics of Deformable Media", Academic Press, New York, 1950.